

# STUDY ON THE APPLICATION OF TLS FOR BRIDGE DEFLECTION INSPECTION IN VIETNAM

Vu Dinh Chieu<sup>a</sup>, Luong Ngoc Dung<sup>a,\*</sup>, Cu Viet Hung<sup>a</sup>, Vu Ngoc Quang<sup>b</sup>, Bui Ngoc Son<sup>a</sup>

<sup>a</sup>*Faculty of Bridges and Roads, Hanoi University of Civil Engineering,  
55 Giai Phong road, Hai Ba Trung district, Hanoi, Vietnam*

<sup>b</sup>*Department of Planning and Urban Transport, University of Transport Technology,  
54 Trieu Khuc road, Thanh Xuan district, Hanoi, Vietnam*

## Article history:

*Received 14/9/2023, Revised 13/12/2023, Accepted 18/12/2023*

---

## Abstract

Inspecting defects, geometric size discrepancies compared to the design profile, and displacement under the load of the bridge structure aims to gather information and current data before putting the bridge into operation. However, the quality of inspection on the structure size performed by traditional methods usually takes time-consuming and potentially unsafe due to difficulties in accessing because the bridge dimension is high and the rugged terrain is challenging, especially with bridges crossing rivers, deep valleys, etc. Therefore, applying modern, effective, and reliable inspection methods is essentially required. The Terrestrial Laser Scanner (TLS) is a technique to quickly and accurately gather topographic data points of objects' surfaces. TLS is applied in many survey fields, including surveying the structure of bridge engineering. To evaluate the effectiveness of applying TLS, the research conducted a determination of the main span P61-62's deflection of the balance casting bridge crossing the Vong intersection of the urban traffic bridge project Ring Road 2, Hanoi city during static load testing. Three methods to determine the deflection of the bridge span structure were implemented: (1) Using dial indicators; (2) Using a total station to measure points reflecting attached to the structure of the bridge girder; (3) Applying TLS to inspect the structure at the time of no load and load. The results led to the conclusion that TLS methodology facilitates the determination of the bridge deflection with acceptable accuracy.

**Keywords:** deflection inspection; TLS; dial indicators; total station; geospatial data process; vertical displacement; Vietnam bridges.

[https://doi.org/10.31814/stce.huce2023-17\(4\)-02](https://doi.org/10.31814/stce.huce2023-17(4)-02) © 2023 Hanoi University of Civil Engineering (HUCE)

---

## 1. Introduction

The requirement to collect data on the structure of old bridges aims to serve renovation, repair, or assess the quality of newly-built bridges and create as-built drawings constantly puts forth challenges in collecting geospatial data. Recently, TLS has been evaluated as effective in the work of quickly and accurately collecting 3D surface spatial data [1–3]. With the main function being the collection of point cloud data, TLS allows the depiction of the spatial surface of the structure with a level of detail that can go up to millions of points on a meter square [4]. Point cloud data is also used to monitor the deformation of construction structures through appropriate analysis methods [5].

One of the initial studies of TLS in bridge engineering was used to determine the overall rotational motion on grid bridges and the deflection of the bridge girder under static load [6]. In evaluating the condition of old bridge projects when there are insufficient documents about the measurements of the structure, Kushwaha et al. [7] used TLS combined with a close-range photogrammetry technique to create point clouds to assess the deformation of the bridge deck structure layers. The outcomes from

---

\*Corresponding author. E-mail address: [dungln@huce.edu.vn](mailto:dungln@huce.edu.vn) (Chieu, V. D.)

the point cloud data of different types of bridges - truss bridge, girder bridge, and cable-stayed bridge - were compared with the laser distometer, having a difference of about 3-5 cm. Cafiso et al. [8] combined TLS and Ground Penetrating Radar techniques to determine the geometry of the structure and the thickness of the asphalt overlay, the bridge deck thickness, and the location of steel reinforcement of an old bridge in Sicily, Italy. The results of evaluating the condition of parts of the bridge surface from this solution are considered valuable, ensuring accuracy, time and cost-effectiveness. Liu et al. [9] used TLS to collect point cloud data to detect and analyze damage to the Beishatan urban bridge in Beijing, China. From point cloud data, 2D, 3D deformation maps and Digital Surface Models (DSM) were built, supporting in determining the areas (locations) of potential damage (areas with large deflection) at the bottom of the bridge. The results of this study affirmed that TLS is an effective technique for detecting potentially damaged areas of bridges.

In terms of monitoring the deformation of bridge structures is also an issue of great interest [10–12]. In this regard, the application of TLS (Terrestrial Laser Scanner) is recognized as effective and suitable for determining the vertical displacement of steel bridge structures in Poland [13]. The research results show that this is an appropriate solution for monitoring and static load testing tasks. Enhancing research on the application of TLS for static load testing of old steel bridges, the authors have also proven that the TLS vertical displacement measurement has a difference of  $\pm 1$  mm compared to the traditional height measurement method with leveling [14]. TLS is also considered useful for determining the elastic line of bridges when conducting dynamic load testing for types of steel bridges, concrete bridges, and cable-stayed bridges [15]. The TLS solution has been proposed to overcome the weaknesses of the deformation observation method for high-speed bridgeheads by precise leveling [16]. A mobile TLS system is arranged on a car to collect point cloud data for three experimental areas. The raw data is denoised in two steps, which are coarse filtering and fine filtering using the plane fitting method based on the experimentally set threshold values. The height of the deformation monitoring point obtained between different TLS measurements differs by  $\pm 1$  mm and  $\pm 2$  mm compared to the results measured by the electronic total station TM50.

The above studies clearly have shown many valuable benefits that TLS brings in evaluating geometry and reconstructing the current situation of various types of old bridge structures in operation. However, the applications of TLS to verify and evaluate the quality of new-build bridge projects have not been mentioned much. In Vietnam, conducting verification of large bridge projects, the bridges with special structures before putting them into operation is a mandatory technical requirement. The main tasks include: (1) Surveying, measuring, and evaluating the current state of the structure [17]; (2) Evaluation of girder concrete quality; (3) Assess the load-bearing ability of bridge structures through load testing experiments. These are the jobs if using TLS techniques and/or combining them with some other techniques like the studies above [7, 9] will help increase efficiency, and safety and ensure the required accuracy.

This paper presents the application of TLS for the assessment of the bearing capacity of the newly built bridges before being put into operation. The process of collecting and processing point cloud data and analyzing bridge deflection during static load testing is mentioned in the article systematically and completely. For comparison with conventional methods, this study contributes to an effective method of utilizing geospatial data for the field of construction structural assessment in Vietnam.

## 2. Material and Methodology

### 2.1. Tested Bridge

The study subject selected is the overpass at the Vong intersection which is a part of the elevated route (urban traffic bridge) of Hanoi city's Ring Road 2 project (Fig. 1). The overpass includes 3

spans arranged according to the diagram 55 m + 90 m + 55 m, using the pre-stressed concrete box girder structure with strutted using slabs, constructed by the balanced cantilever method. The bridge girder width is 18.7 m with three vertical walls. The height of the box girder changes according to the parabolic path with the girder height at the closure segment and cast on the scaffolding is 2.687 m, and near the pier top is 5.687 m. The width of the box girder's bottom slab is 7 m.



Figure 1. The overpass at Vong intersection which is a part of Hanoi city's Ring Road 2 project

To assess the load-bearing capacity of the bridge girder structure before it is put into operation, static and dynamic load tests are carried out. The static load test work is performed for the mid-span between P61-P62 and the side span P62-P63. For the main static test P61-P62, 8 concrete mixing trucks are used, each with a whole load of about 27-30 tons. The experiment vehicle layout includes two cases which are concentric and eccentric load positions (Fig. 2). For each case, three measurements are carried out (the vehicle enters and exits the load position three times).



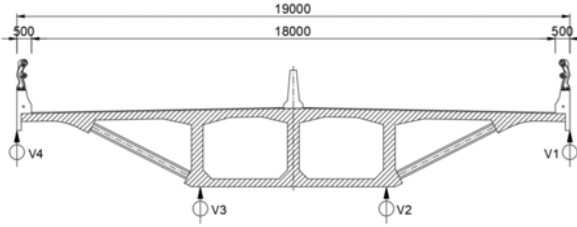
Figure 2. The truck arrangement diagram for static load tests of the P61-P62 span, illustrating potential load scenarios

## 2.2. Methodology

To measure the deflection of the bridge under a static load with eight trucks as mentioned above, our study used 3 measurement methods: (1) Installing dial indicators, (2) Using total station, and (3) Applying TLS to collect data. The solution using a dial indicator or a total station can only measure the bridge's deflection at some predefined positions, while TLS allows gathering point cloud data.

### a. Using dial indicators

Using the dial indicator is a conventional method to determine the bridge deflection during the static load test. Four dial indicators are vernier dial gauges arranged in the middle of spans P61-P62 under the bridge girder as shown in Fig. 3. The numbers read on the dial are performed in two cases no load and with a load (when arranging trucks on the bridge). The difference between these two measured values is the deflection at the point where the device is mounted. The disadvantage of this method is that there may be errors due to the human eye reading the dial and the elasticity of the suspension system of the measuring device.



(a) The position of dial indicators



(b) The on-site installation process

Figure 3. Deflection inspection using dial indicators

### b. Using a total station

The total station with the function of measuring distance based on the principle of mirrorless reflection has high accuracy. This allows the total station to be applied to determine the elevation of points according to the principle of trigonometric height measurement, the following formula (1).

$$\begin{aligned} h &= D * \tan V + j - g \\ H_i &= H_M + h \end{aligned} \quad (1)$$

where  $h$  is the elevation difference between the station and point,  $D$  is the horizontal distance,  $V$  is the vertical angle,  $j$  is the height of the total station,  $g$  is the height of the reflector,  $H_i$  is the elevation of the point and  $H_M$  is the elevation of the station.

The bridge deflection then is calculated following the total station methodology by the formula (2)

$$V_i = H_i^{Ini} - H_i^{Cur} \quad (2)$$

in which  $V_i$  is the deflection value,  $H_i^{Ini}$  is the elevation at the no-load case and  $H_i^{Cur}$  is the elevation at the load test case.

The Trimble C3 total station and paper reflections were selected in the study (Fig. 4). The accuracies of distance and angle measurements are  $2 + 2$  ppm and  $1''$ , respectively.

Keeping the total station stable during the load test process so that the values of the station elevation ( $H_M$ ) and station height ( $j$ ), in formula (1), are unchanged components. In addition, the height reflector ( $g$ ) is considered zero because the paper reflectors were attached to the survey points (Fig. 4). The accuracy of the elevation of the points ( $H_i$ ) depends completely on the accuracy of quantities  $D$  and  $V$ . The accuracy of quantity  $D$  depends on the distance from the station to the measurement point, in practice with the longest distance within 100 m, this accuracy is achieved within  $\pm 2.2$  mm. For quantity  $V$ , to ensure the accuracy requirement, at each point, conduct three times at both left and right readings and then take the average value. Parallely, choosing the position to set the station so that the vertical angle value  $V$  is minor than 15 degrees.



Figure 4. Installation of total station and paper reflectors' position for deflection inspection

Although it is impossible to avoid sources of error due to the accuracy of the equipment and the environment affecting the elevation of the survey points, with the measures implemented, these sources of error are always stable for all the measuring points during the load testing process. In formula (2), the bridge deflection is calculated as the difference between the elevation values of the measuring points at the unloaded time and the loaded time. Therefore, these uniform errors once again reduce the impact on the accuracy of the elevations by the subtraction of the calculation formula. This helps us obtain more reliable results (according to the principle of accuracy being less than three times the allowable limit).

#### c. Using TLS

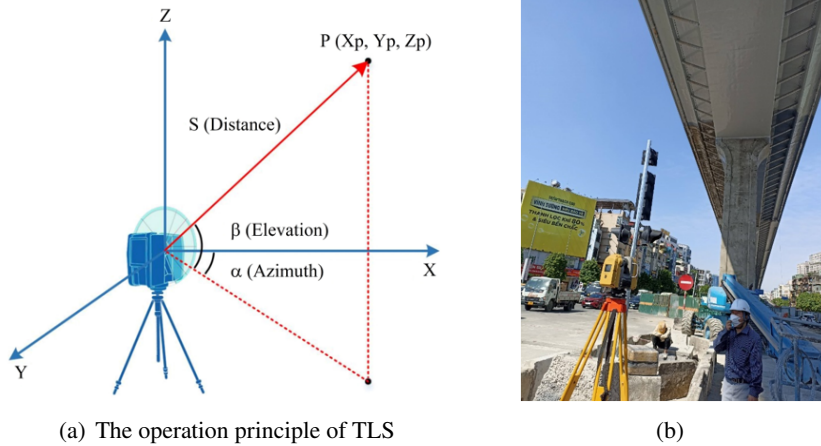


Figure 5. Deflection inspection using TLS

TLS is a non-prism laser measurement technique used to acquire 3D point cloud data. From the instrument station, a laser girder is emitted toward the scanning object. Each reflected girder will yield the values of distance  $S$ , vertical angle  $\beta$ , and azimuth angle  $\alpha$  of a spatial point, as shown in Fig. 5(a). In this case, the spatial coordinates component  $(X_P, Y_P, Z_P)$  in the coordinate system with the instrument station as the origin can be determined according to formula (3) [18].



$$\begin{aligned}
 X_P &= S \cos \beta \cos \alpha \\
 Y_P &= S \cos \beta \sin \alpha \\
 Z_P &= S \cos \beta
 \end{aligned}
 \tag{3}$$

TOPCON GLS-2200 is the TLS device used for scanning and measuring the bridge deflection in this study, as shown in Fig. 5(b). In addition to its scanning range of up to 500 m with a distance accuracy of  $\pm 3.1$  mm and angle accuracy of 6 seconds, this TLS device allows for the collection of point cloud density at a frequency of 120,000 points per second. After processing through MAGNET Collage software, it is possible to obtain surfaces with an accuracy of  $\pm 1$  mm [19].

In reality, it is hard to determine the exact positions of the same surveyed points in point clouds from different scans. So the determination of displacements by comparing these points directly is impossible. It requires allocation of parts of the object in the process of modeling the parts of the point cloud data [5]. Determining displacements therefore based on the differences between two point clouds is commonly applied. The relationship between point clouds is determined by registering them in a common coordinate system, usually done using the ICP algorithm [20]. After a registration process, the point clouds are then divided into clusters which are used to calculate the geometric displacements based on the average distance strategies between corresponding clusters. This can be done by computing the distances between matching point pairs from both point clouds, or by computing the maximum distance from a set of distances of nearby points. Alternatively, displacements can be determined simply by the coordinate differences between the centers of corresponding point cloud clusters in scanning cycles [21]. A more complex and improved method can use geometric principles by modeling regression planes [4].

Based on the principle of comparing the coordinate differences between the centroids of each cluster in different load conditions, the Height Inspection function of Coprocess software allows for extraction, analysis of vertical displacement, and determination of deflection. The process of performing deflection inspection and analysis of the structure uses data from point clouds described in a workflow of Fig. 6.

### 3. Experimental results

#### 3.1. Girder deflection using dial indicators

Four dial indicators (marked V1, V2, V3, and V4) were installed respectively at the positions of the right-wing, the right bottom, the left bottom, and the left-wing of girder following the route direction of the P61-P62 main span (Fig. 3(a)). The data from four dial indicators are recorded with 3 readings per measurement and the average value is taken. Table 1 describes the average readings and

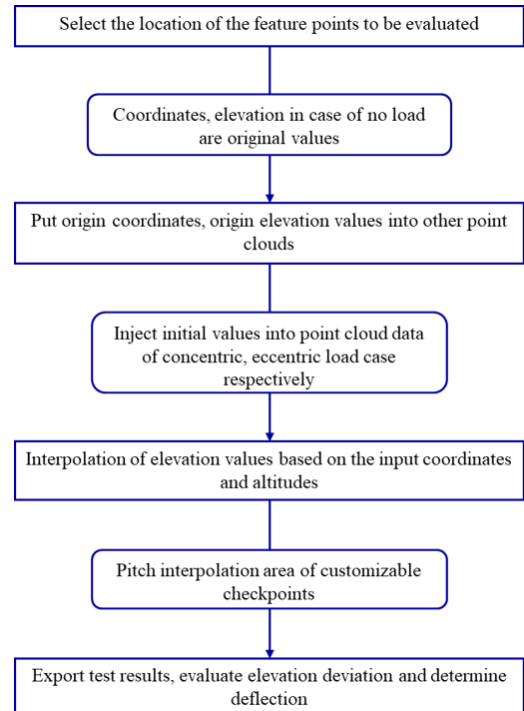


Figure 6. Workflow of point cloud data processing to determine the deflection

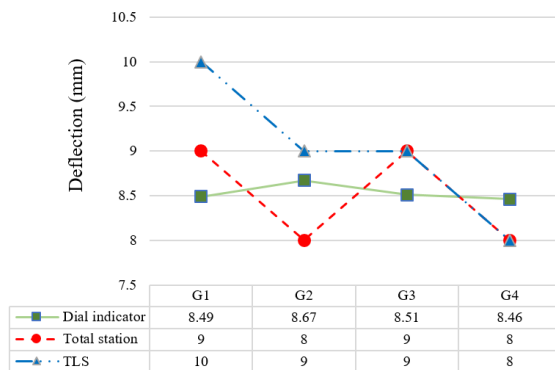
the girder deflection is calculated by subtraction of average readings of the no-load case during both tests of concentric load and eccentric load.

Table 1. P61-62 span deflections using dial indicators

Marker	Position	Concentric load		Eccentric load	
		Average reading V	Deflection (mm)	Average reading V	Deflection (mm)
V1	Right-wing	848.83	8.49	1065.90	10.66
V2	Right bottom	867.17	8.67	874.87	8.75
V3	Left bottom	851.03	8.51	776.60	7.77
V4	Left-wing	845.90	8.46	583.00	5.83

The graph representing the girder deflection (Fig. 7) shows that the girder deflection under the concentric load is relatively uniform. This reflected the proper functioning of the structure suffering the impact of central load, the largest deflection value at the right bottom position is 8.67 mm. In the case of the eccentric load applied towards the right side, the girder deflection at the right wing and bottom positions is larger than that of the left side, with the maximum deflection value of 10.66 mm occurring at the position of the right-wing.

### 3.2. Beams deflection using total station



(a) Concentric load

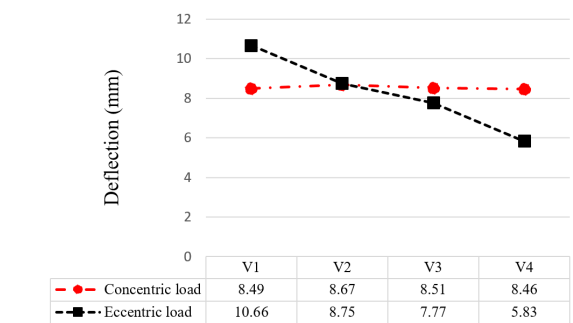
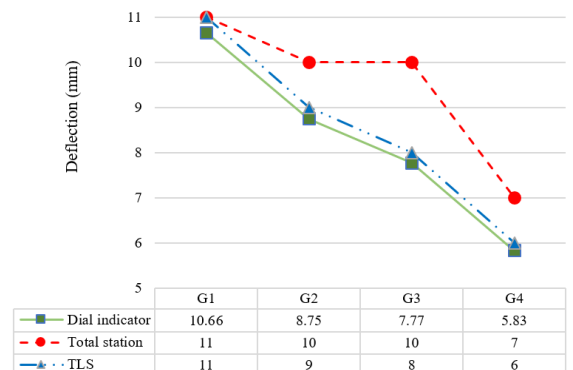


Figure 7. Girder deflection values of the P61-P62 main span using dial indicators



(b) Eccentric load

Figure 8. Girder deflection values of the P61-P62 main span using the total station compared to Dial indicator and TLS methods

Determining the deflection using total station, four paper targets (marked G1, G2, G3 and G4) are also simultaneously located at the corresponding positions of four dial indicators (Fig. 4). The girder deflections are calculated according to formula (2) and shown in the chart of Fig. 8 (red line). Compared with the dial indicator results (green line), there are differences of about  $\pm 0.5$  mm and

$\pm 2.0$  mm in the case of the concentric load and eccentric load, respectively. It has been mentioned that these deviations are due to the accuracy of the total station and they are within one-third of the allowable limit. Therefore, this result fully satisfies the accuracy requirements for determining the deflection of bridge structures according to technical standards, and it also accurately reflects the behavior of the structure under the influence of both central and eccentric load. The results of girder deflection using TLS are discussed in detail in the following subsection.

### 3.3. Girder deflection using TLS

Unlike the two previous methods, the TLS methodology does not determine a specific position on the girder structure but relies on the analysis of point clouds for analysis. The TLS method requires two basic steps: collecting, processing raw data and analyzing the vertical displacement of point cloud clusters to determine the bridge deflection. In our experiment, point cloud data was collected using the GLS-2200 device in unloaded, concentrically loaded, and eccentrically loaded epoques. Then, the data was processed to eliminate noise using the MAGNET Collage Ver2.3 software, which provided us with point cloud data in each loading case (Table 2).

Table 2. Scanning information in loading cases after noise processing

File name (situation)	Number of scanning (point)	Scanning area (m <sup>2</sup> )	Min density (point/m <sup>2</sup> )	Max density (point/m <sup>2</sup> )	Average density (point/m <sup>2</sup> )
1KT_SCN0002 (no load)	1974106	1589	2	73060	1242,357
1KT_SCN0003 (concentric load)	1972601	1586	4	68158	1243,759
1KT_SCN0006 (eccentric load)	1973189	1587	1	69880	1243,345

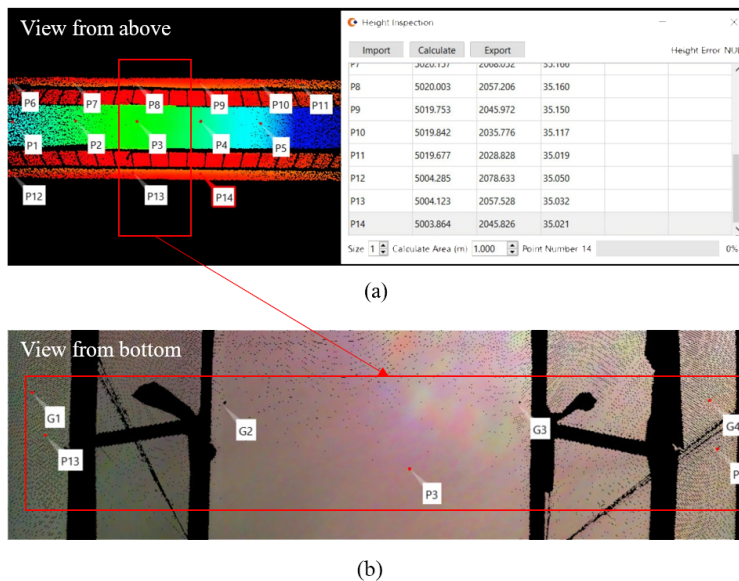


Figure 9. Registering and processing geospatial data of point clouds, (a) the results of 14 inspection points of the unloaded case, and (b)  $G_i$  points derived from the total station after registering point cloud data

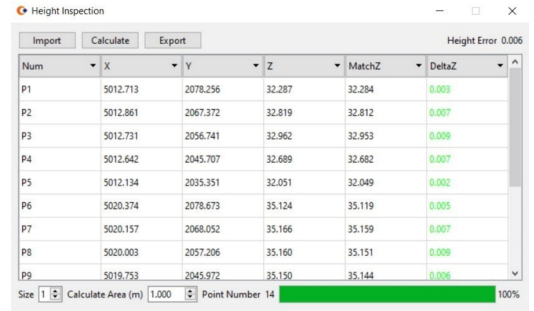
With the Height inspection function in the Coprocess software, after registering the positions of inspection points on the main span surface in the unloaded case, the elevation of points  $P_i$  (Fig. 9(a)) is interpolated from points within the area of a one-meter square. The elevations of points  $P_i$  in the unloaded case are chosen as the reference values to determine the bridge deflections. Then, the



corresponding obtained elevations under each load case are subtracted from the reference elevations to calculate the girder deflection at each position.

Applying this principle, the coordinates of four targets ( $G_i$ ) derived from the total station were registered into point cloud data of the unloaded, concentric and eccentric loads (Fig. 9(b)). The elevations of  $G_i$  points were then interpolated and extracted to calculate girder deflections. The girder deflections derived from TLS data were presented in Fig. 8, these results were close to the deflection results using the total station in the concentric load and the dial indicator data in the eccentric load. All of the discrepancies are within  $\pm 1.0$  mm, demonstrating the suitability of the TLS method to collect geospatial data and also to ensure technical accuracy during deflection testing.

As mentioned earlier, the use of point cloud data provides us with the advantage of evaluating the deflection of the whole girder. In this study, deflection data from fourteen  $P_i$  points, which were distributed across the entire girder (Fig. 9(a)), were extracted. The original coordinates of the  $P_i$  points derived from the unloaded case were registered into the point clouds of concentric and eccentric load cases, to ensure the correct positioning of the inspection points. Fig. 10 displays an example of the elevations of fourteen inspection points that were interpolated from the point clouds of the concentric load test. These obtained elevations then are subtracted from the reference elevations of the unloaded case to calculate deflection. Table 3 shows the elevation results of the  $P_i$  points in each unloaded, concentric load and eccentric load case, as well as the elevation differences (the girder deflections) of load cases.



Num	X	Y	Z	MatchZ	DeltaZ
P1	5012.713	2078.256	32.287	32.284	0.003
P2	5012.861	2067.372	32.819	32.812	0.007
P3	5012.731	2056.741	32.962	32.953	0.009
P4	5012.642	2045.707	32.689	32.682	0.007
P5	5012.134	2035.351	32.051	32.049	0.002
P6	5020.374	2078.673	35.124	35.119	0.005
P7	5020.157	2068.052	35.166	35.159	0.007
P8	5020.003	2057.206	35.160	35.151	0.009
P9	5019.753	2045.972	35.150	35.144	0.006

Figure 10. The elevation interpolation for the  $P_i$  points of the concentric load case

Table 3. Elevation of inspection points and deflections in the case of the concentric load and the eccentric load

Position	Unload Elevation (m)	Concentric load Elevation (m)	Eccentric load Elevation (m)	Concentric load Deflection (mm)	Eccentric load Deflection (mm)
P1	32.287	32.280	32.279	-7	-8
P2	32.819	32.811	32.812	-8	-7
P3	32.962	32.953	32.953	-9	-9
P4	32.689	32.682	32.682	-7	-7
P5	32.051	32.049	32.050	-2	-1
P6	35.124	35.119	35.121	-5	-3
P7	35.166	35.159	35.159	-7	-7
P8	35.160	35.151	35.155	-9	-5
P9	35.150	35.144	35.144	-6	-6
P10	35.117	35.111	35.113	-6	-4
P11	35.019	35.016	35.014	-3	-5
P12	35.050	35.046	35.049	-4	-1
P13	35.032	35.027	35.026	-5	-6
P14	35.021	35.014	35.013	-7	-8

The results in Table 3 show that the smallest deflections, in both centric and eccentric load tests,

have occurred at the P5 point. The deflections at points P3, P8, and P13 (near the location of  $G_i$  points) give us the largest values and this is rather reasonable to regard with the results of  $G_i$  points discussed above. With the availability of point cloud data, we have the capability to accurately assess and evaluate the deflection at any specific position along the girder during the static load test.

#### 4. Discussion and future direction

Experiment results to determine the deflection at the P61-P62 main span have some slight differences among the three used methods. Compared with the dial indicators and total station for concentric load test, the TLS method exhibits differences in the range of 0.46 mm to 1.51 mm. When subjected to the eccentric load test, these differences lie within the range of 0.34 mm to 2.33 mm. These discrepancies can be ascribed to the contrasting methods of data accumulation and treatment amongst the devices involved. Nevertheless, it is observable that such errors remain lesser in magnitude, being between three to five times less than the deflection values, thereby satisfying the stipulated technical standards. While variations in deflection values amongst the trio of methodologies persist, they uniformly provide an accurate portrayal of the structural behavior under loading conditions.

Assessing work efficiency, using the dial indicators is a reliable traditional method for determining deflection in static load testing. However, it has no time effectively for installation and equipment operation. These devices especially require strict occupational safety during installing equipment for large-span structures. The total station equipment has an easier operation for the inspection of bridge deflection. However, this method also determines vertical displacement for individual points and hardly describes the entire structural surface. On the other hand, the TLS method provides point cloud data with high point density, which has helped simulate the entire surface of the bridge structure during static load testing. From the point cloud data, the deflection of the bridge span can be calculated to meet technical requirements. Additionally, the point cloud data also provides the ability to construct cross-sectional planes and deflection contour maps over the whole structure surface. It is an effective method for determining bridge deflection, the TLS methodology helps increase safety, efficiency, and work productivity. However, it still has limitations in terms of cost and requires a more complex data processing process than the above two methods.

In addition, one of the recent approaches of TLS to bridge infrastructure is to create a 3D digital twin model to support bridge inspection tasks that are safer, cheaper, more reliable, and less cumbersome compared to traditional direct assessment methods [22]. In this research direction, Masoud Mohammadi and colleagues [23] have also proposed the monitoring/inspection of bridge structures based on accurate 3D model extraction, as well as the integration of non-geometric information with structural components for managing bridge assets and developing a Bridge Information Model (BrIM) system. Future research suggests the development of Bridge Management Systems (BMS) that include Artificial Intelligence (AI) [24, 25], decision support systems [20], and Internet of Things (IoT) [26], not only to collect real-time information but also to evaluate and prioritize tasks. Asset managers can benefit from real-time decision-making, propose strategic plans, and distribute tasks to other team members. Over the past decade, TLS technology has been well-known for its accurate and fast data collection, making it perfectly suitable for creating and updating information models like BrIM. However, research still lacks automated and productive methods for creating high LoD (Level of Detail) 3D models [27], as well as suitable AI solutions for real-time monitoring of the health of structures and updating bridge information models (BrIM) [18, 28].

#### 5. Conclusions

In determining the bridge deflection during static load testing, the study used three methodologies such as dial indicators, total station, and Terrestrial Laser Scanning. All three methods meet the

technical requirements and render similar results, correctly reflecting the working conditions of the bridge structure during load tests. The results of determining the main span deflection P61-P62 by all three methods were approximately 11 and 9 mm in concentric and eccentric load tests, respectively. Comparing the variations among the three solutions, the deflection values are three to five times the differences. This reflects the acceptable level of confidence when applying TLS to replace the deflection meter and electronic total station method. This application aims to enhance the efficiency of identifying bridge deflection.

## Acknowledgments

This research has been supported by a grant for the basic research project (No.16-2023/KHXD) from Hanoi University of Civil Engineering. Part of the experiments' support was provided by the Institute of Geodesy Engineering Technology.

## References

- [1] Rashidi, M., Mohammadi, M., Sadeghlou Kivi, S., Abdolvand, M. M., Truong-Hong, L., Samali, B. (2020). [A decade of modern bridge monitoring using terrestrial laser scanning: review and future directions](#). *Remote Sensing*, 12(22):3796.
- [2] Tran, H. H., Pham, N. T. (2021). [Building 3D model for the deep vertical shaft in Nui Beo coal mine using Terrestrial laser scanning technology](#). *Journal of Mining and Earth Sciences*, 62(5a):128–134.
- [3] Nguyen, N. V., Vo, D. N. (2016). The possibility applying of Terrestrial Laser Scanner 3D for construction-mining management in underground mines. *Journal of Mining and Earth Sciences*, 57: 65–73.
- [4] Erdélyi, J., Kopáčík, A., Kyrinovič, P. (2020). [Spatial data analysis for deformation monitoring of bridge structures](#). *Applied Sciences*, 10(23):8731.
- [5] Neuner, H., Holst, C., Kuhlmann, H. (2016). Overview on current modelling strategies of point clouds for deformation analysis. *Allgemeine Vermessungs-Nachrichten: AVN; Zeitschrift für alle Bereiche der Geodäsie und Geoinformation*, 123(11-12):328–339.
- [6] Fuchs, P. A., Washer, G. A., Chase, S. B., Moore, M. (2004). [Applications of laser-based instrumentation for highway bridges](#). *Journal of Bridge Engineering*, 9(6):541–549.
- [7] Kushwaha, S. K. P., Pande, H., Raghavendra, S. (2018). [Digital documentation, bridge deck linearity deformation and deck thickness measurement using terrestrial laser scanner \(TLS\) and Close Range Photogrammetry \(CRP\)](#). *ISPRS Annals of the Photogrammetry, Remote Sensing and Spatial Information Sciences*, IV–5:47–51.
- [8] Cafiso, S., Di Graziano, A., Goulías, D., Mangiameli, M., Mussumeci, G. (2020). [Implementation of GPR and TLS data for the assessment of the bridge slab geometry and reinforcement](#). *Archives of Civil Engineering*, 66(1):297–308.
- [9] Liu, X., Wang, P., Lu, Z., Gao, K., Wang, H., Jiao, C., Zhang, X. (2019). [Damage detection and analysis of urban bridges using terrestrial laser scanning \(TLS\), ground-based microwave interferometry, and permanent scatterer interferometry synthetic aperture radar \(PS-InSAR\)](#). *Remote Sensing*, 11(5):580.
- [10] Thanh, T. P., Hung, T. V., Hung, C. V., Phat, N. T., Son, N. H., Nhung, V. T. H., Tuan, N. N. (2021). [Stress-Strain Monitoring Of Long-Span Arch Bridges During Construction Using Vibration Wire Strain Gauge System In Vietnam](#). *Journal of Science and Technology in Civil Engineering (JSTCE) - HUCE*, 15(7V):13–25. (in Vietnamese).
- [11] Quang, V. N., Chieu, V. D., Hoa, P. T. T. (2022). An experiment study of inspection and monitoring bridge using ground laser scanner total station. *Sci. J. Archit. Constr. Sci.*, 45:65–69.
- [12] Pham, C. V., Le, C. V., Nguyen, L. Q., Le, H. T. T., Nguyen, A. T., Nguyen, H. V., Nguyen, H. V. (2023). [Monitoring tram rail transport in underground coal mines using terrestrial laser scanning](#). *Journal of Mining and Earth Sciences*, 64(2):91–100.
- [13] Gawronek, P., Makuch, M., Mitka, B., Gargula, T. (2019). [Measurements of the vertical displacements of a railway bridge using TLS technology in the context of the upgrade of the polish railway transport](#). *Sensors*, 19(19):4275.

- [14] Gawronek, P., Makuch, M. (2019). [TLS measurement during static load testing of a railway bridge](#). *ISPRS International Journal of Geo-Information*, 8(1):44.
- [15] Artese, S., Zinno, R. (2020). [TLS for dynamic measurement of the elastic line of bridges](#). *Applied Sciences*, 10(3):1182.
- [16] Liu, M., Sun, X., Wang, Y., Shao, Y., You, Y. (2020). [Deformation measurement of highway bridge head based on mobile TLS data](#). *IEEE Access*, 8:85605–85615.
- [17] Cao, C. X., Le, C. V., Vo, D. N., Ta, H. T. T., Ngo, C. S., Dang, T. T. (2022). [UAV and TLS point cloud integration for the surface plant infrastructure of underground coal mines](#). *Journal of Mining and Earth Sciences*, 63(4):13–23.
- [18] Wu, C., Yuan, Y., Tang, Y., Tian, B. (2021). [Application of terrestrial laser scanning \(TLS\) in the architecture, engineering and construction \(AEC\) industry](#). *Sensors*, 22(1):265.
- [19] TOPCON. [GLS-2200 Series 3D Laser Scanner](#). Accessed June 17, 2023.
- [20] Wunderlich, T., Niemeier, W., Wujanz, D., Holst, C., Neitzel, F., Kuhlmann, H. (2016). Areal Deformation Analysis from TLS Point Clouds-The Challenge/Flächenhafte Deformationsanalyse Aus TLS-Punktwolken-Die Herausforderung. *Allg. Vermess. Nachr*, 123:340–351.
- [21] Girardeau-Montaut, D., Roux, M., Marc, R., Thibault, G. (2005). Change detection on points cloud data acquired with a ground laser scanner. *International Archives of Photogrammetry, Remote Sensing and Spatial Information Sciences*, 36(3):W19.
- [22] Mohammadi, M., Rashidi, M., Mousavi, V., Karami, A., Yu, Y., Samali, B. (2021). [Quality Evaluation of Digital Twins Generated Based on UAV Photogrammetry and TLS: Bridge Case Study](#). *Remote Sensing*, 13(17):3499.
- [23] Mohammadi, M., Rashidi, M., Mousavi, V., Yu, Y., Samali, B. (2022). [Application of TLS Method in Digitization of Bridge Infrastructures: A Path to BrIM Development](#). *Remote Sensing*, 14(5):1148.
- [24] Liu, J., Mohammadi, M., Zhan, Y., Zheng, P., Rashidi, M., Mehrabi, P. (2021). [Utilizing Artificial Intelligence to Predict the Superplasticizer Demand of Self-Consolidating Concrete Incorporating Pumice, Slag, and Fly Ash Powders](#). *Materials*, 14(22):6792.
- [25] Yu, Y., Rashidi, M., Samali, B., Mohammadi, M., Nguyen, A. (2021). Computer vision-based classification of cracks on concrete bridges using machine learning techniques. In *Proceedings of the 10th International Conference on Structural Health Monitoring of Intelligent Infrastructure (SHMII-10)*, International Society for Structural Health Monitoring of Intelligent . . . , 1707–1712.
- [26] Zinno, R., Artese, S., Clausi, G., Magarò, F., Meduri, S., Miceli, A., Venneri, A. (2018). *Structural Health Monitoring (SHM)*. Springer International Publishing, 225–249.
- [27] Le, H. T. T., Nguyen, T. V., Pham, L. T., Tong, S. S., Nguyen, L. H., Vo, O. D. (2022). [Combined use of Terrestrial Laser Scanning and UAV Photogrammetry in producing the LoD3 of 3D high building model](#). *Journal of Mining and Earth Sciences*, 63(4):24–34.
- [28] Mohammadi, M., Rashidi, M., Yu, Y., Samali, B. (2023). [Integration of TLS-derived Bridge Information Modeling \(BrIM\) with a Decision Support System \(DSS\) for digital twinning and asset management of bridge infrastructures](#). *Computers in Industry*, 147:103881.